ChemComm
Chemical Communications

Accepted Manuscript

This article can be cited before page numbers have been issued, to do this please use: K. Zhang, M. Sun, H. Song, Y. Su and Y. Lv, *Chem. Commun.*, 2020, DOI: 10.1039/D0CC00313A.

ROYAL SOCIETY OF CHEMISTRY

rsc.li/chemcomm

View Article Online
DOI: 10.1039/D0CC00313A

COMMUNICATION

Synergistic chemiluminescence nanoprobe: Au clusters-Cu^{2+}-induced chemiexcitation of cyclic peroxides and resonance energy transfer

Received 00th January 20xx,
Accepted 00th January 20xx

DOI: 10.1039/x0xx00000x

Kexin Zhang,[a] Mingxia Sun, [b] Hongjie Song,[a] Yingying Su[b] and Yi Lv* [ab]

An interesting chemiluminescence (CL) phenomenon of cyclic peroxides originated from Tetrahydrofuran hydrogen peroxide (THF-HPO) in the presence of BSA-stabilized Au NCs (Au@BSA NCs) was found for the first time. In this CL system, Au@BSA NCs can greatly accelerate the decomposition of THF-HPO, and then chemiluminescence resonance energy transfer (CRET) occurs between excited dioxetane derivatives and Au@BSA NCs, yielding enhanced CL emission which can be futher enhanced more than 10 times by the adding of copper ions. Based on this, a synergistic CL nanoprobe with a special signal amplification strategy was developed.

Chemiluminescence (CL), deriving from chemiexcitation process in special chemical reaction, has been an attractive topic of intensive research due to its extremely low background signal. However, for diverse analytical applications, improving sensitivity and stability of CL is still an ongoing challenge.[1] Thus, nanoparticle-assisted novel CL system[2] and signal amplification technique[3] have become growing areas of interest in recent years because of their powerful contribution to the excellent sensitivity and stability for CL methods.

A cyclic peroxide species, an unstable unit, subsequently forms intermediate with high energy, which emits blue light.[4] Furthermore, as a source of excited products, cyclic peroxide species can tune the emission color by energy transfer to suitable acceptor and induce CL amplification. Based on this, Shabat and his coworkers developed a kind of dioxetane – fluorogenic dye conjugates which was successfully applied to bioimaging.[5] Afterwards, stimuli-responsive self-immolative polymers which innately assimilated chemiexcitation in a domino-like fragmentation to produce amplified CL was developed by them.[6] Unfortunately, most of the cyclic peroxide based CL probes need complex synthesis due to instability. More importantly, due to aggregation-caused CL quenching and small Stokes shift, fluorescent dyes as CL energy acceptors become an intractable problem.[7] In this case, nanomaterials and semiconducting polymer dots are currently attracting considerable attention as an excellent candidate in CRET process.[8]

Nanoclusters, designed with the protection groups, has large specific surface area and extraordinary optical property. Accordingly, nanoclusters is regarded as an excellent enzymatic catalyst and luminophore to amplify the CL and imaging.[9] Lin's group observed a significantly enhancement induced by the catalysis and unique the surface plasmon coupled of Zn/Cu@BSA NCs in the $NaHCO_3$-H_2O_2 system.[10] Lu's group exploited Au NCs as CL luminophores in the Bis(2,4,6-trichlorophenyl) Oxalate (TCPO)-H_2O_2 system, which exhibited a remarkable enhancement due to the aggregation.[11] Taking into account these merits of nanoclusters, a novel nanoclusters based CL system with greatly signal amplification can be developed by coalescing the above effects. Herein, we reported Au clusters-induced synergistic enhanced chemiluminescence nanoprobe with a double signal amplification strategy. Firstly, BSA-stabilized Au NCs could greatly promote the chemiexcitation of cyclic peroxides which were produced from the decomposition of Tetrahydrofuran hydrogen peroxide (THF-HPO).[12] Simultaneously, with the large Stokes shifts and greatly energy-transfer efficiency of Au@BSA NCs, CRET occurred between excited dioxetane derivatives and Au@BSA NCs, yielding enhanced CL emission. Surprisingly, it was further enhanced by copper ions.

The Au@BSA NCs was synthesized via a facile method as reported. As shown in Fig. S1, the optical spectrum, XPS, Fourier transform infrared (FTIR), and far-UV circular dichroism (CD) analysis strongly suggested the formation of Au@BSA NCs, which were accordant with the previously reported results.[13]

A new CL phenomenon was illustrated in Fig. 1A, upon injecting Au@BSA NCs solution into THF solution containing THF-HPO, without any external light excitation, an evident luminescence signal was obtained, and the intensity was pronouncedly intensified more than ten times when adding copper ions. Interestingly, the signal peak was rapidly produced in several seconds until it reached a maximum value, and the emission could last for a long time over 600 s (Fig. 1B). Meanwhile, the CL of the above mixture system was dependent

[a] Key Laboratory of Green Chemistry & Technology, Ministry of Education, College of chemistry, Sichuan university, Chengdu, Sichuan, 610064, China.
[b] Analytical & Testing Center, Sichuan University, Chengdu 610064, China. E-mail: lvy@scu.edu.cn; Fax: +86-28-85412798; Tel: +86-28-85412798.
†Electronic Supplementary Information (ESI) available: Preparation methods, spectrum and analytical performance. See DOI: 10.1039/x0xx00000x

View Article Online
DOI: 10.1039/D0CC00313A

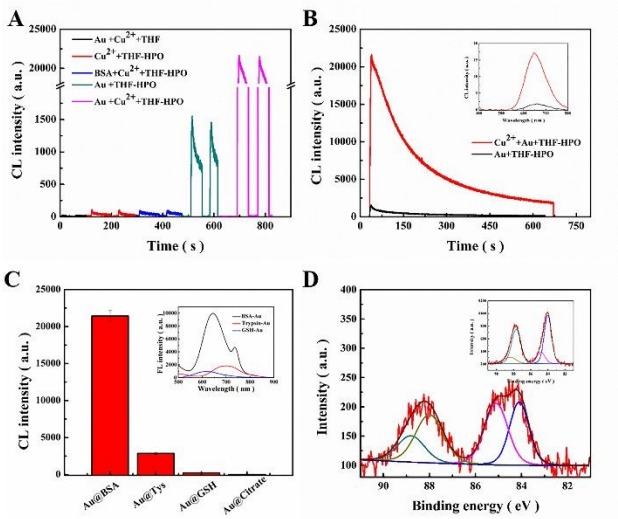

Fig. 1 (A)Replicate CL signals of the THF- Au@BSA NCs − Cu^{2+} (blank), THF-HPO - Cu^{2+} (red),and THF-HPO -BSA − Cu^{2+}(blue curve), THF-HPO- Au@BSA NCs (dark green curve) and THF-HPO - Au@BSA NCs − Cu^{2+} (purple curve) systems. (B)Kinetic curves of CL of THF-HPO - Au@BSA NCs and THF-HPO- Au@BSA NCs–Cu^{2+} systems. The inset of (B) displayed the CL spectrum of the above systems. (C) The CL signals of THF-HPO with different kinds of gold nanoparticles. The inset of (C) was the FL spectrum of gold nanoparticles. (D) XPS spectra of Au 4f for Au@BSA NCs after the reaction with THF-HPO. The insert of (D) was the XPS spectra of Au@BSA NCs before the reaction.

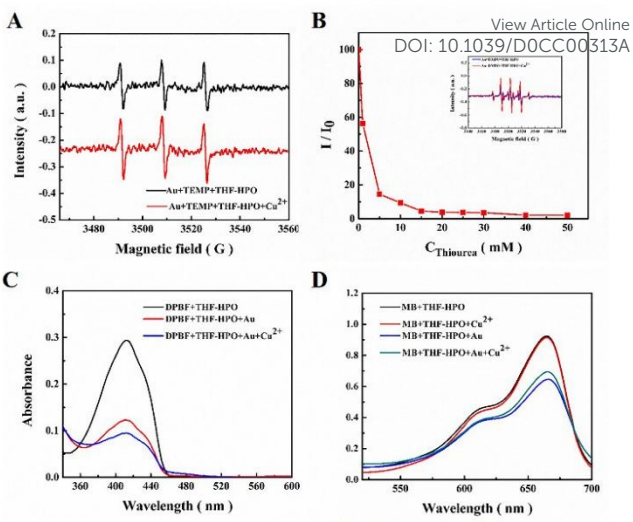

Fig. 2 Evaluation of •OH and $^1O_2$ production in the CL reactions. (A and C) ESR spectra and the absorbance of DPBF to study the $^1O_2$ generated in the Au@BSA NCs-THF-HPO and Au@BSA NCs-THF-HPO-Cu^{2+} system. (B) Effects of thiourea as •OH scavenger on the Au@BSA NCs-THF-HPO-Cu^{2+} system. The insert of(B) is the ESR spectra of •OH generated in the CL systems. (D) MB trapping measurements of •OH generated in the Au@BSA NCs-THF-HPO and Au@BSA NCs- THF-HPO -Cu^{2+} system. Conditions: DMPO 50 mM, TEMP 100 mM, DPBF 5 mg L^{-1}, MB 5 mg L^{-1}, Au@BSA NCs 0.04 mM, THF-HPO 1 mM, Cu^{2+} 2×10^{-4} M.

of pH (Fig. S3D). It suggested that this system had a highest CL in acidic condition (pH=2). Under the same condition, a control experiment was performed. As shown in Fig. 1A, THF-HPO-Cu^{2+} and BSA-THF-HPO-Cu^{2+} systems both have an ultra-weak CL, Au@BSA NCs-THF-Cu^{2+} has almost no CL signal compared with Au@BSA NCs-THF-HPO-Cu^{2+} system. Meanwhile, no similar CL signal was recorded when gold nanoparticles with different active sites and FL intensity (Fig.1C). All these results indicated that Au@BSA NCs and THF-HPO played important roles in the CL phenomenon. This conclusion could also be demonstrated by altering the mixing orders of reagents (Fig. S2A). The highest CL intensity created with the injection of the mixture of Au@BSA NCs and Cu^{2+} into THF-HPO by contrast to that the lowest CL intensity was detected after adding Cu^{2+} to the mixture of THF-HPO and Au@BSA NCs, and a slight weaker signal was obtained when Cu^{2+} was added before Au@BSA NCs into THF-HPO. Subsequently, we measured the CL wavelength of Au@BSA NCs-THF-HPO and Au@BSA NCs-Cu^{2+}-THF-HPO systems by a fluorescence spectrophotometer with the excitation lamp was off. As shown in the insert of Fig. 1B, there was only one peak and the maximum emission was located at 650 nm, which was overlapped with the FL spectrum of the Au@BSA NCs. The overlapping nature of the spectra confirmed that the reaction of Au@BSA NCs-THF-HPO and Au@BSA NCs-Cu^{2+}-THF-HPO system could generate excited-state Au@BSA NCs.

To elucidate the influence of Au@BSA NCs on CL reaction, the optical properties and morphology of Au@BSA NCs after the CL process (Fig. S3) were investigated. The UV-vis absorption spectrum was measured to identify the conformational behavior of BSA in Au NCs after CL reaction, which showed that there was an evident change in absorption intensity in system. The same result was also confirmed by the DLS measures in Fig.S3B. These results seemed to be consistent with the previous reports.[14] Simultaneously, the decreased fluorescence intensity of the Au@BSA NCs after reacting with THF-HPO, and X-ray photoelectron spectroscopy data all indicated that the Au centers was oxidized. As shown in Fig. 1D, in the presence of the THF-HPO, the ratio of the $Au4f_{7/2}$ peaks at 85.0 eV and 84.0 eV, which corresponded to Au (1) and Au (0), was increased than that of original Au nanoclusters.[15] All of these characteristic results indicated that there was an oxidation reaction between the Au@BSA NCs and THF-HPO.

Generally, the active oxygen radicals were easily produced from the unstable peroxides in the presence of Au nanoparticles.[16] According to the previous reports, we wondered whether the CL phenomenon was induced from the reactive oxygen species. Firstly, the relations between dissolved oxygen and the CL reaction was investigated. The solution of CL system was bubbled with N_2 or O_2 for 30 min before the CL reaction, respectively, Fig. S4 showed there was slightly decreased after bubbled with O_2, which reflected that the dissolved oxygen did not implicated the CL emission. Then, we studied the effects of different active oxygen radical scavengers on the CL emission.[17] As shown in Fig. S5, the CL intensity obviously decreased and even totally quenched when eliminated $^1O_2$, •OH, and $•O_2^-$, respectively. Likewise, electron spin resonance (ESR) spectroscopy and UV-vis absorption were employed to investigate whether or not there were $^1O_2$ and •OH radicals in this CL system. 2,2,6,6-Tetramethyl-4-Piperidoe (TEMP) and 1,3-diphenylisobenzofuran (DPBF) were usually used to verify the existence of $^1O_2$.[18] TEMP could capture $^1O_2$ to generate nitroxide radical (TEMPO), which has a typical spectrum. According to Fig. 2A, there were significant ESR signals corresponding to TEMPO in the Au@BSA NCs-THF-HPO and Au@BSA NCs-THF-HPO-Cu^{2+} system. Moreover, the

increasing intensity of TEMPO verified that more $^1O_2$ were produced when adding Cu^{2+} in the CL system. This was possibly because Cu^{2+} could easily promote the formation of $•O_2^-$, and $•O_2^-$ was unstable in aqueous solution to convert to $^1O_2$. DPBF could react with $^1O_2$ undergoing a Diels-Alder 1,4-cycloaddition, which was used as probe molecule to identify $^1O_2$ generated in the CL process.[19] From the UV-vis analysis (Fig. 2C), a strong absorption peak around 410 nm, ascribed to the unique absorption of DPBF, was observed when adding DPBF into the Au@BSA NCs-THF-HPO and Au@BSA NCs-THF-HPO-Cu^{2+} system. And it was consistent with the results of EPR that the increasing absorption peak at 410 nm in the presence of Au@BSA NCs. At the same time, thiourea as a frequently •OH radical inhibitor was added into the CL system, and the CL intensity even totally quenched (Fig. 2B). In particular, due to the super oxidation capacity of THF-HPO, the strong 1:1:1 triplet signal assigned to the oxidation peak of DMPO was clearly displayed in the insert of Fig.2B. The generation of •OH was also affirmed by spectrophotometry when methylene blue was served as indicator.[20] When methylene blue reacted with •OH to form hydroxylated methylene blue, the absorption peak at 620 nm was decreased in the CL system (Fig. 2D). Therefore, the above experiments proved that •OH and $^1O_2$ were present in this CL system and had an important effect on the CL emission.

We further analyzed whether the active species trigged the CL reaction. As shown in Fig. 3A, the various active species including $^1O_2$, •OH, $•O_2^-$, RO• and ClO^- were used to confirm the speculation. However, no obvious signal could be initiated by $•O_2^-$, •OH or ClO^-. The relatively obvious emission was

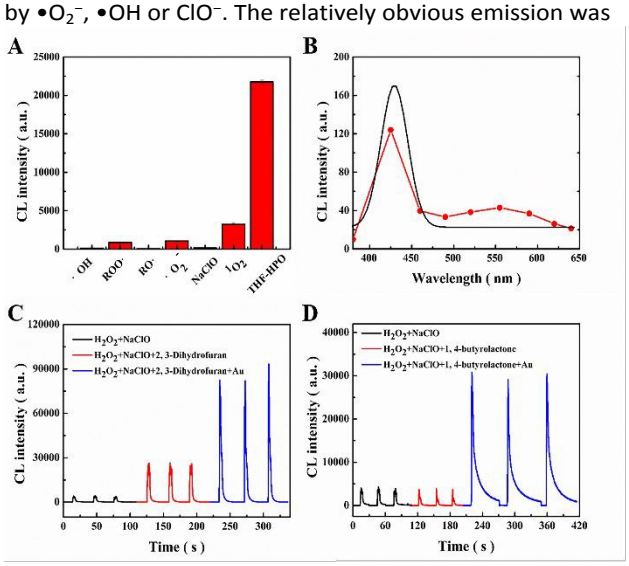

Fig. 3 (A) The CL intensity of Au@BSA NCs towards different kinds of ROS. (B) CL spectra of THF-HPO-$•O^{2-}$ systems. The CL curve of (C) the 2,3-Dihydrofuran-$^1O_2$-Au@BSA NCs and (D) 1,4-butyrolactone-$^1O_2$-Au@BSA NCs system. Conditions: H_2O_2 and NaClO 10 mM, (C) Au@BSA NCs 0.4 μM, (D) Au@BSA NCs 4 μM.

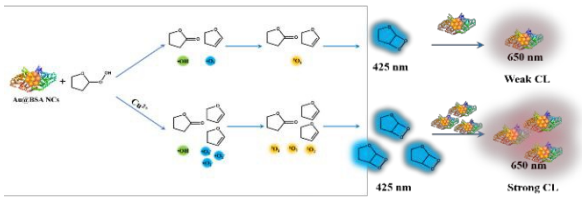

Fig. 4 Proposed CL mechanism of the Au@BSA NCs-THF-HPO-Cu^{2+} system.

obtained when $^1O_2$ was introduced into Au@BSA NCs-Cu^{2+} system, but the same phenomenon arose from BSA-Cu^{2+}. From the above, the proposed system exhibited no emission with individual free radicals. Besides, the CL signal of Au@BSA NCs in the existence of •OH mixed with $•O_2^-$ was studied. In the control system, H_2O_2, $ONOO^-$ and tert-Butyl hydroperoxide (TBHP) were performed as a source of •OH and $•O_2^-$. The existence of $•O_2^-$ and •OH radicals in these reactions were monitored by the UV - vis absorption. The results pointed out that the similar equivalent of radicals was generated in these systems (Fig. S6). Unfortunately, no similar CL curve was detected after adding Au@BSA NCs into the above peroxides, which firmly illustrated that the commonly radicals could not induce Au@BSA NCs emitted and the CL emission could not be derived from the electron-hole recombination CL process.

Based on the previous reports, peroxides can oxidize any tryptophan metabolites to produce an emission species with the CL peak centered at 558 nm.[10] In the view of such results, we speculated chemiluminescence resonance energy transfer might occur a from the tryptophan residue luminophore to the Au@BSA NCs receptors. Considering this possibility, various oxidizing agents instead of THF-HPO applied in the CL reaction were investigated. However, very weak emission was recorded while other oxidizing agents were used in the presence of the Au@BSA NCs, depicted as in Fig. S7. Furthermore, the synchronous fluorescence spectrum of tryptophan before and after CL reactions was monitored to substantiate the above. The changes of tryptophan in the existence of H_2O_2 or THF-HPO were displayed in Fig. S8, which implied that the similar equivalent of tryptophan was consumed in the reactions and could not occur the CRET. Interestingly, similar CL phenomena were observed when Au@BSA NCs reacted with other ether peroxides (Fig. S9). According to the above data, the CL system might have special reactive intermediates which dominated the CL emission.

In order to further study the probable mechanism of the CL system, $•O_2^-$ acted as the reactant for the THF-HPO with a static injection system and the emitters were investigated using high-energy cutoff filters. It could be seen from Fig. 3B that only one peak at 425 nm was detected, which was identical to the intermediate (C_2O_4*) of TCPO-H_2O_2 system.[21] Surprisingly, it had been reported that the 2,3-Dihydrofuran could react with $^1O_2$ to form the dioxetane derivatives, which decomposed to emit around 420 nm.[21, 22] Therefore, we presumed that the similar emitters might generate in such CL system, and it further happened CRET from the intermediate to the Au@BSA NCs. To further verify the validity of CRET, we investigated the CL emission of 2,3-Dihydrofuran-$^1O_2$-Au@BSA NCs. As expected, this system enabled successful CRET. As illustrated in Fig. 3C, upon adding only 0.4 μM Au@BSA NCs into the 2,3-Dihydrofuran-$^1O_2$ system, an obviously increased CL intensity was detected. The same result was obtained in the 1,4-butyrolactone-$^1O_2$ system(Fig. 3D). In addition, HPLC and FT-IR were applied to study the feature of the THF-HPO. After the CL reaction, the obvious absorption peak at about 1780 cm^{-1} assigned to C=O was appeared in FT-IR, which indicated the product had carbonyl groups. The similar phenomenon was

verified by the GC-MS (Fig. S10C). At about 2.315 min and 12.563 min, peaks belonged to 2,3-Dihydrofuran and 1,4-butyrolactone were observed, respectively. All data manifested the Au@BSA NCs induced the dioxetane derivatives generation, which further trigged CRET to amplification.

On the basis of the above results, a proposed CL mechanism was illustrated as described in Fig. 4. The active sites of Au@BSA NCs promoted the decomposition of THF-HPO to generate •OH, $•O_2^-$, 1,4-butyrolactone and 2,3-Dihydrofuran. $^1O_2$ formed simultaneously from the combination of •OH and $•O_2^-$. When introducing Cu^{2+}, Cu^{2+} cooperated with Au@BSA NCs and broke up THF-HPO specifically to produce more $•O_2^-$,[23] and unstable $•O_2^-$ in aqueous solution converted into $^1O_2$. Then, $^1O_2$ reacted with 1,4-butyrolactone and 2,3-Dihydrofuran to produce the excited dioxetane derivatives. Particularly, this special excited intermediate was formed on the surface of Au@BSA NCs and could trigger the highly efficient collision, which promoted the decomposition and light emission at 425 nm. This process could persistently generate excited intermediate. Meanwhile, the emitters transfer energy to the Au@BSA NCs equipped with prolong fluorescence to generated excited-state nanoclusters. Finally, intense and long-lasting CL emission with a peak at 650 nm was generated due to the energy release of excited-state Au@BSA NCs (Fig. S11). Considering the superior analytical performance of the CL system, we explored it as a CL probe for the quantitative analysis of THF-HPO. The CL responses of the proposed probe toward THF-HPO with different concentrations were tested under the optimal conditions. As illustrated in Fig. S12, there was linear correlation between the CL signals and the concentration of THF-HPO from 500 nM to 20 μM and from 40 μM to 3.5 mM. The limit of detection (LOD) for THF-HPO was 37.71 nM (S/N = 3). Meanwhile, the CL response to Cu^{2+} was examined in the CL system.

Conclusions

In conclusion, we describe a synergistic chemiluminescence phenomenon of Au@BSA NCs-Cu^{2+} and cyclic peroxides originated from THF-HPO. First, Au@BSA NCs-Cu^{2+} was utilized to stimulate the decomposition of ether peroxides to generate excited dioxetane derivatives, accompanied by light emission. Then CRET occurs between excited dioxetane derivatives and Au@BSA NCs-Cu^{2+}, yielding greatly enhanced CL emission. With the special signal amplification strategy, a highly sensitive and selective CL nanoprobe towards ether peroxides was constructed. We postulate the special signal amplification strategy could be extended to more CL systems to design new nanoprobes with high sensitivity.

The authors gratefully acknowledge financial support from the National Natural Science Foundation of China (No. 21874094 & 21405107). We also thank Dr. Shuguang Yan in Analytical & Testing Center of Sichuan University for technical assistance.

Conflicts of interest

There are no conflicts to declare.

Notes and references

View Article Online
DOI: 10.1039/D0CC00313A

1 K. Aslan and C. D. Geddes, *Chem. Soc. Rev.*, 2009, **38**, 2556-2564; H. Chen, L. Lin, H. Li and J.-M. Lin, *Coord. Chem. Rev.*, 2014, **263-264**, 86-100; Y. Su, D. Deng, L. Zhang, H. Song and Y. Lv, *TrAC, Trends Anal. Chem.*, 2016, **82**, 394-411.
2 H. Song, Y. Su, L. Zhang and Y. Lv, *Luminescence*, 2019, **34**, 530-543; S. N. Shah and J. M. Lin, *Adv. Colloid Interface Sci.*, 2017, **241**, 24-36; D. L. Giokas, A. G. Vlessidis, G. Z. Tsogas and N. P. Evmiridis, *TrAC, Trends Anal. Chem.*, 2010, **29**, 1113-1126.
3 S. Bi, H. Zhou and S. Zhang, *Chem. Sci.*, 2010, **1**, 681; X. Huang, L. Li, H. Qian, C. Dong and J. Ren, *Angew. Chem.*, 2006, **118**, 5264-5267; P. Li, L. Liu, H. Xiao, W. Zhang, L. Wang and B. Tang, *J. Am. Chem. Soc.*, 2016, **138**, 2893-2896.
4 M. Vacher, I. Fdez Galvan, B. W. Ding, S. Schramm, R. Berraud-Pache, P. Naumov, N. Ferre, Y. J. Liu, I. Navizet, D. Roca-Sanjuan, W. J. Baader and R. Lindh, *Chem. Rev.*, 2018, **118**, 6927-6974.
5 N. Hananya, A. Eldar Boock, C. R. Bauer, R. Satchi-Fainaro and D. Shabat, *J. Am. Chem. Soc.*, 2016, **138**, 13438-13446.
6 S. Gnaim and D. Shabat, *J. Am. Chem. Soc.*, 2017, **139**, 10002-10008.
7 C. Zong, J. Wu, Y. Zang and H. Ju, *Chem. Commun.*, 2018, **54**, 11861-11864.
8 E. S. Lee, V. G. Deepagan, D. G. You, J. Jeon, G. R. Yi, J. Y. Lee, D. S. Lee, Y. D. Suh and J. H. Park, *Chem. Commun.*, 2016, **52**, 4132-4135; C. L. Shen, Q. Lou, C. F. Lv, J. H. Zang, S. N. Qu, L. Dong and C. X. Shan, *Adv. Sci.*, 2019, **6**, 1802331.
9 K. Zhao, W. Shen and H. Cui, *J. Mater. Chem. C,*2018, **6**, 6549-6555; Y. Xie, Y. Xianyu, N. Wang, Z. Yan, Y. Liu, K. Zhu, N. S. Hatzakis and X. Jiang, *Adv. Funct. Mater.*, 2018, **28**, 1702026.
10 H. Chen, L. Lin, H. Li, J. Li and J.-M. Lin, *ACS Nano*, 2015, **9**, 2173-2183.
11 L. Zhang, N. He and C. Lu, *Anal. Chem.*, 2015, **87**, 1351-1357.
12 B. Division, *Nature*, 1948, 4108; S. Rashid, B. A. Bhat, S. Sen and G. Mehta, *Tetrahedron Lett.*, 2016, **57**, 5355-5358.
13 J. Xie, Y. Zheng and J. Y. Ying, *J. Am. Chem. Soc.*, 2009, **131**, 888-889; Y. M. Fang, J. Song, J. Li, Y. W. Wang, H. H. Yang, J. J. Sun and G. N. Chen, *Chem. Commun.*, 2011, **47**, 2369-2371.
14 L. Jin, L. Shang, S. Guo, Y. Fang, D. Wen, L. Wang, J. Yin and S. Dong, *Biosens. Bioelectron.*, 2011, **26**, 1965-1969.
15 R. Tian, S. Zhang, M. Li, Y. Zhou, B. Lu, D. Yan, M. Wei, D. G. Evans and X. Duan, *Adv. Funct. Mater.*, 2015, **25**, 5006-5015.
16 K. L. Lin, T. Yang, F. F. Zhang, G. Lei, H. Y. Zou, Y. F. Li and C. Z. Huang, *J. Mater. Chem. B,* 2017, **5**, 7335-7341; C. Duan, H. Cui, Z. Zhang, B. Liu, J. Guo and W. Wang, *J. Phys. Chem. C,* 2007, **111**, 4561-4566.
17 Y. Zheng, X. Dou, H. Li and J. M. Lin, *Nanoscale*, 2016, **8**, 4933-4937; M. Sun, L. Wu, H. Ren, X. Chen, J. Ouyang and N. Na, Anal. Chem., 2017, **89**, 11183-11188;
18 H. Liu, Y. Su, D. Deng, H. Song and Y. Lv, *Anal. Chem.*, 2019, **91**, 9174-9180; M. Sun, D. Deng, K. Zhang, T. Lu, Y. Su, Y. Lv, *Chem. Commun.*, 2016, **52**,11259-11262; L. He, Z. W. Peng, Z. W. Jiang, X. Q. Tang, C. Z. Huang and Y. F. Li, *ACS Appl. Mater. Interfaces,* 2017, **9**, 31834-31840.
19 H. Liu, M. Sun, Y. Su, D. Deng, J. Hu and Y. Lv, *Chem. Commun.*, 2018, **54**, 7987-7990.
20 X. Dou, Q. Zhang, S. N. A. Shah, M. Khan, K. Uchiyama and J. M. Lin, *Chem. Sci.*, 2019, **10**, 497-500; C. J. Miller, A. L. Rose and T. D. Waite, *Anal. Chem.*, 2011, **83**, 261-268.
21 M. Matsumoto, K. Hamaoka, Y. Takashima, M. Yokokawa, K. Yamada, N. Watanabe and H. K. Ijuin, *Chem. Commun.*, 2005, 808-810.
22 H. M. A. N. Masakatsu Matsumoto, *Chem. Commun.*, 1998, 2319-2320.
23 L. Yang, M. Zeng, Y. Du, L. Wang and B. Peng, *Luminescence*,

2018, **33**, 1268-1274; N. S. A. S. Shinji MURAi, 1963, **36**, 527-530.

View Article Online
DOI: 10.1039/D0CC00313A

Graphical Abstract